Electromagnetic Flow Meters Achieve High Accuracy in Industrial Applications

By Li Ke and Colm Slattery

Introduction

Industrial applications ranging from oil refineries to vending machines require precision measurements of temperature, pressure, and flow to control complex and simple processes. Within the food industry, for example, the accurate control of flow when filling bottles and cans can directly influence profits, so flow measurement errors must be minimized. Similarly, custody transfer applications, such as the exchange of raw and refined petroleum between tanks and tankers in the oil industry, require high-accuracy measurements. This article presents an overview of flow meter technologies, focusing on electromagnetic flow meters, which are among the most accurate for liquid flow measurement.

Figure 1 shows a basic process control system that uses a flow meter and actuator to control liquid flow rate. At the lowest level, process variables such as temperature, flow rate, and gas concentration are monitored via an input module that is typically part of a programmable logic controller (PLC). The information is processed locally by a proportional-integral-derivative (PID) loop. Using this information, the PLC sets the output to control the process in a steady state. Process data, diagnostics, and other information can be passed up to the operations level, and commands, parameters, and calibration data can be passed down to the sensors and actuators.

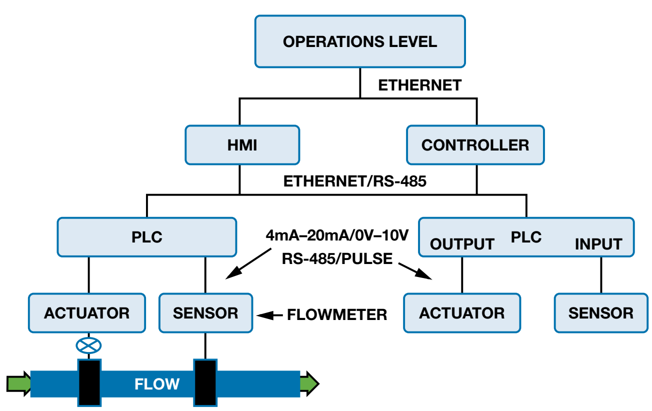

Figure 1. Basic system for measuring and controlling liquid flow rate.

Many different technologies are used to measure flow rate, including differential pressure, Coriolis, ultrasound, and electromagnetic. Differential pressure flow meters are the most common, but they are sensitive to pressure changes in the system. Coriolis flow meters can provide the highest accuracy, up to 0.1%, but they are large and expensive. Ultrasonic flow meters are reasonably small and low cost, but have limited accuracy (0.5% typical). Ultrasonic flow meters use a noninvasive measurement technique that improves reliability and minimizes degradation of the sensing element over time, but they can't be used with dirty or contaminated liquids.

Electromagnetic flow meters also offer noninvasive sensing. They can be used with acidic, alkali, and ionized fluids with electrical conductivities ranging from 10 S/m to 10^{-6} S/m, and with clean, dirty, corrosive, erosive, or viscous liquids and slurries, but are not suited for use in hydrocarbon or gas flow measurement. They can achieve relatively high system accuracies (0.2%) at low and high volume flow rates with a minimum diameter of about 0.125 inches and a maximum volume of about 10 cubic feet, and the readings remain repeatable at even slower velocities. They can measure bidirectional flow, either upstream or downstream. Table 1 compares several common flow meter technologies.

Electromagnetic flow meters use Faraday's law of electromagnetic induction, which states that a voltage will be induced in a conductor moving through a magnetic field. The liquid serves as the conductor; the magnetic field is created by energized coils outside the flow tube. The magnitude of the induced voltage is directly proportional to the velocity and type of conductor, the diameter of the tube, and the strength of the magnetic field, as shown in Figure 2.

Mathematically, we can state Faraday's law as $E = kBLV$

where V is the velocity of a conductive fluid, B is the magnetic field strength, L is the spacing between the pickup electrodes, E is the voltage measured across the electrodes, and k is a constant. B, L, and k are either fixed or can be calibrated, so the equation reduces to $E \propto V$.

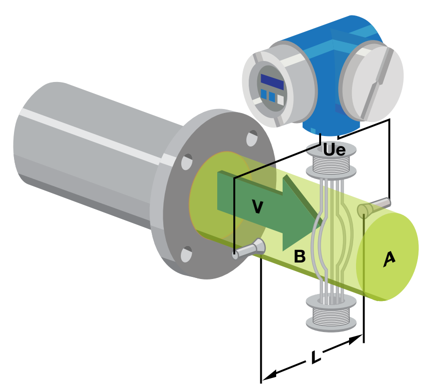

Figure 2. Electromagnetic flow meter.

Table 1. Industrial Flow Meter Technologies

	Electromagnetic	Differential Pressure	Ultrasound	Coriolis
Measurement Technique	Faraday's law of electromagnetic induction	Differential: capacitive or bridge based	Transducer/sensor cross correlation, time to digital, Doppler	Differential phase
Average Accuracy	0.2%–1%	0.5%–2%	0.3%–2%	0.1%
Average Cost	\$300–\$1000	\$300–\$1000	\$300–\$1000	\$3000–\$10000
Advantages	No moving parts Useful with corrosive liquids Bidirectional flow measurement	No moving parts Versatile, can be used for liquids/gases	No moving parts Versatile, can be adopted post-installation	Versatile, can be used for nearly all liquids/gases Independent of pressure and temperature

A current passing through the field coils of a solenoid generates a controlled magnetic field. The particular excitation waveform is an important aspect of electromagnetic flow meters, and many types are used, including low-frequency rectangle wave, power line frequency sine wave, dual frequency wave, and programmable pulse width. Table 2 shows various sensor coil excitation waveforms.

Most applications use a low-frequency dc rectangle to excite the sensor coil at 1/25, 1/16, 1/10, 1/8, 1/4, or 1/2 of the power line frequency (50 Hz/60 Hz). Low-frequency excitation uses a constant amplitude, alternating direction current to achieve low zero drift. The direction of current flow is switched with a transistor or MOSFET H-bridge. When SW1 and SW4 are on, and SW2 and SW3 are off (Figure 3a), the sensor coil is excited in the positive phase; and the constant current enters EXC+ and exits EXC–. When SW1 and SW4 are off, and SW2 and SW3 are on (Figure 3b), the sensor coil is excited in the negative phase; and the constant current enters EXC– and exits EXC+.

Table 2. Sensor Excitation Types, Waveform, and Features

Excitation Type	Waveform	Features
DC current excitation	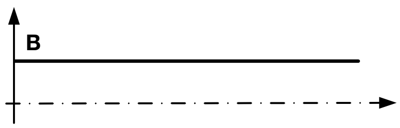	Used since 1832. Used in liquid state metal flow measurement in nuclear energy industry. No polarization, but eddy current.
AC sine wave	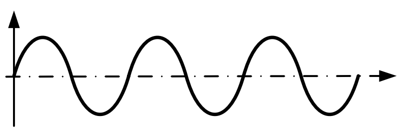	Used since 1920. Commercialized in 1950. Low polarization voltage, electromagnetic disturbance, zero-point drift.
Low frequency dc rectangle	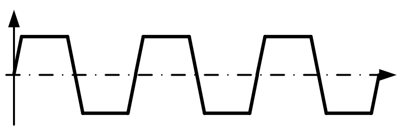	Used since 1975. Frequency is 1/16–1/2 of power line frequency. Low zero-point drift, less immune to noisy serofluid.
Tri-state low frequency dc	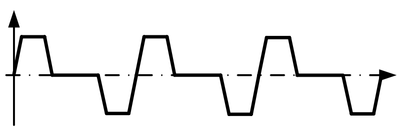	Used since 1978. Calibrate zero point during absence of excitation current. Low power. Duty cycle is 1/2 that of rectangle.
Dual frequency	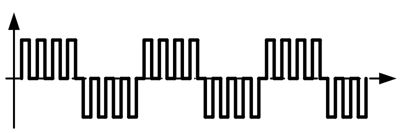	Modulate 1/8 power-line frequency with a higher frequency. Can minimize serofluid noise. Low zero-point drift. Fast response. Complex operation.
Programmable pulse width	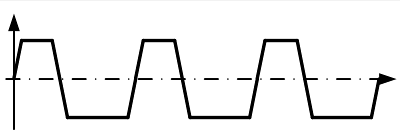	Use microprocessor to control excitation pulse width and frequency. Immune to serofluid noise.

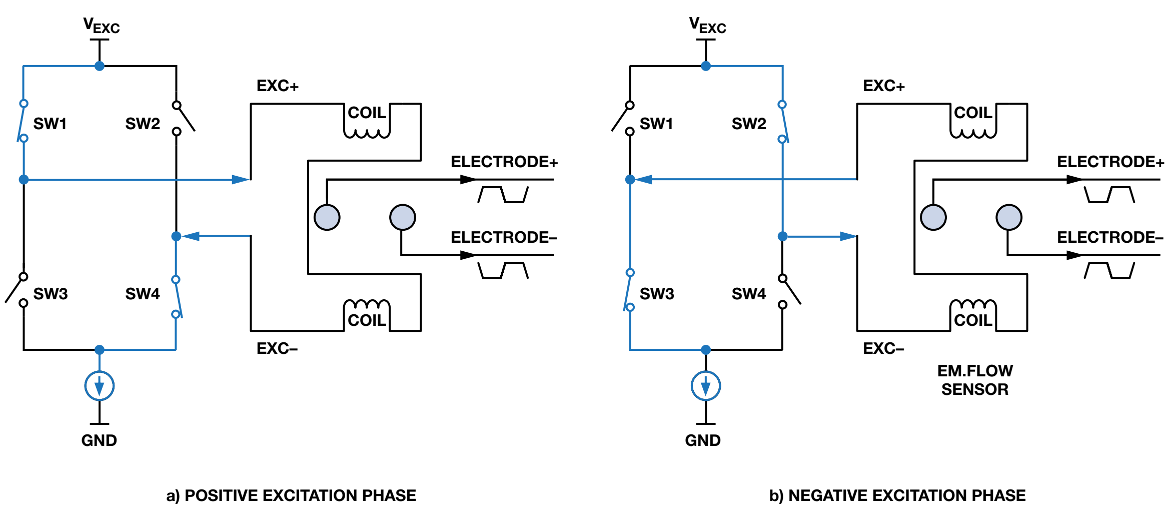

Figure 3. An H-bridge controls the sensor coil excitation phase.

Excitation currents for electromagnetic flow meters tend to be quite large relative to other flow techniques, with 125 mA to 250 mA covering a majority of ranges for line-powered flow meters. Current up to 500 mA or 1 A would be used for larger diameter pipes. Figure 4 shows a circuit that can generate a precision 250 mA sensor coil excitation. The ADR3412 8-ppm/°C voltage reference provides a 1.2-V set point to bias the current.

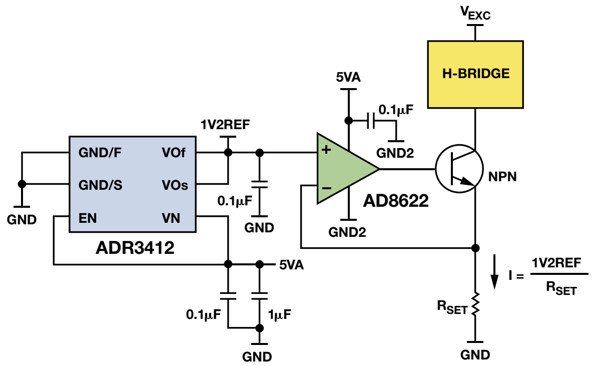

Figure 4. Linear regulated current sink.

Although this traditional method for current excitation using the reference, amplifier, and transistor circuit provides good performance with low noise, it suffers from significant power loss due to the linear drop of the large current across a large voltage. It thus needs heat sinks that add to system cost and area. A constant current sink with switch-mode power supply is becoming a more popular way to excite the sensor coil. Figure 5 shows the ADP2441 synchronous step-down dc-to-dc regulator configured to provide a constant current output. This technique eliminates the losses in standard current sinks and greatly improves system performance.

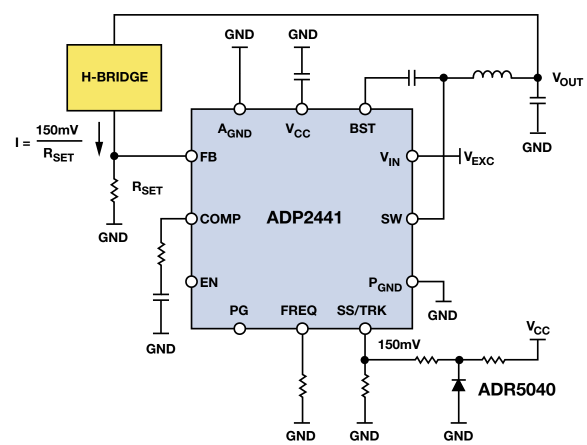

Figure 5. Switch-mode constant current excitation circuit.

Higher power systems use a current sense diagnostic function to monitor current variation over load, power supply, time, and temperature; and can also detect open sensor coils. The AD8219 current shunt amplifier can be used to monitor the excitation current with 60 V/V gain and 0.3% accuracy over an 80-V common-mode range. An isolated current amplifier using the AD7400A isolated Σ-Δ modulator and the AD8646 rail-to-rail op amp is shown in Figure 6. The AD7400 output is processed through a 4th-order low-pass filter to reconstruct the sensed output.

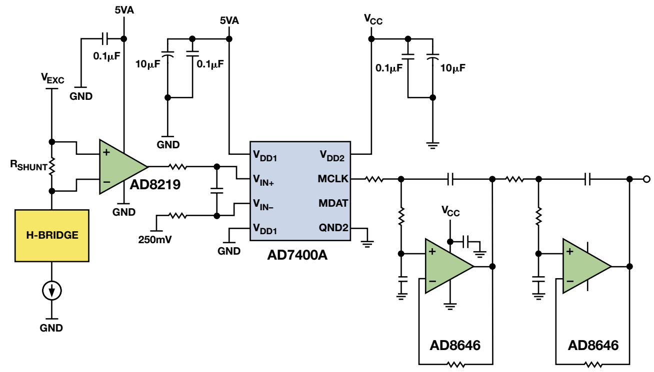

Figure 6. Isolated excitation current monitoring.

The electrode or sensing element is also an important consideration. The two main measurement techniques are capacitive, with electrodes mounted outside of the tube; or, more commonly, with the electrodes inserted through the tube, flush with the liquid.

Many different material options are available, each with unique characteristics including temperature drift, corrosion rate, and electrode potential. The best combination uses a high-temperature material (>100°C) with a low corrosion rate (<0.02 inches per year). Table 3 shows some representative sensor materials and their standard voltage potentials.

Table 3. Sensor Materials and Voltage Potentials

Metal	Standard Voltage Potential (V)	Metal	Standard Voltage Potential (V)
Magnesium	–2.34	**Nickel**	–0.25
Beryllium	–1.70	**Lead**	–0.126
Aluminum	–1.67	**Copper**	+0.345
Manganese	–1.05	**Silver**	+0.800
Zinc	–0.762	**Platinum**	+1.2
Chromium	+0.71	**Gold**	+1.42

Platinum is a good example of a high-quality electrode material; it has corrosion rates of less than 0.002 inches per year and can operate in environments up to 120°C. The 1.2-V electrode potential of platinum is relatively high, however, and will become the common-mode voltage (CMV) that needs rejection at the sensor output. Stainless steel electrodes have only a couple hundred millivolts of CMV, so the common mode can be more easily rejected. Stainless steel material is widely used with non-corrosive fluids.

Equal potential should appear on both electrodes if they use the same material and have the same surface condition. In reality, however, the polarization potential fluctuates slowly as a low-frequency ac signal because of physical friction or electrochemical effects between the fluid and electrodes. Any mismatch would also show up as differential-mode noise. The bias voltage, together with the electrode potential, presents a common-mode voltage of a few hundred millivolts to about 1 V to the first stage amplifier input, so the electronics must have adequate common-mode rejection. Figure 7 shows the one-electrode potential from a differential system with 0.28 V_{DC} bias and 0.1 V_{P-P} noise on #316 stainless steel electrodes installed on a 50 mm diameter water pipe.

Figure 7. Electrode potential in differential system with 0.28 V_{DC} bias and 0.1 V_{P-P} common-mode noise.

Typical flow rates are in the 0.01 m/s to 15 m/s range—a 1500:1 dynamic range. The sensitivity of a typical line-powered electromagnetic flow meter is 150 µV/(m/s) to 200 µV/(m/s). Thus, a 150 µV/(m/s) sensor will provide a 3 μV_{P-P} output with a 0.01 m/s bidirectional flow. For a 2:1 signal-to-noise ratio, the total input-referred noise should not exceed 1.5 μV_{P-P}. The flow rate changes quite slowly in the dc to low frequency range, so the 0.1 Hz to 10 Hz noise bandwidth is critical. In addition, the sensor's output resistance can be quite high. To satisfy these requirements, the front-end amplifier must have low noise, high common-mode rejection, and low input bias current.

The sensor's common-mode output voltage is attenuated by common-mode rejection of the front-end amplifier. With 120 dB CMR, the 0.28 V_{DC} bias is reduced to 0.28 μV_{DC}. This offset can be calibrated out or removed by ac coupling the signal. The ac component appears as noise at the amplifier output, degrading the minimum detectable level. With 120 dB CMR, the 0.1 V_{P-P} is reduced to 0.1 μV_{P-P}.

The sensor output resistance varies from a few tens of ohms to 107 Ω depending on the electrode type and fluid conductivity. To minimize loss, the input impedance of the front-end amplifier must be far greater than the output resistance of the sensor. A JFET or CMOS input stage with high input resistance is required. The low bias current and low offset current of the front-end amplifier are key parameters to minimize the current noise and common-mode voltage. Table 4 shows the specifications of several recommended front-end amplifiers.

Table 4. Specifications of Representative Instrumentation Amplifiers

Model	**Gain**	**Z_{IN}**	**CMR (dB min) DC to 1 kHz, G = 10**	**1/f Noise (μV_{P-P})**	**I_{BIAS} (pA)**	**Power Supply (V)**
AD620	1 to 10,000	10^9 Ω || 2 pF	100	0.55	500	±2.3 to ±18
AD8220	1 to 1000	10^{13} Ω || 5 pF	100	0.94	10	±2.25 to ±18
AD8221	1 to 1000	10^{11} Ω || 2 pF	110	0.5	200	±2.3 to ±18
AD8228	10, 100	10^{11} Ω || 2 pF	100	0.5	400	±2.3 to ±18
AD8421	1 to 10,000	3×10^{10} Ω || 3 pF	114	0.5	100	±2.5 to ±18

Figure 8 shows a flow meter using the AD8228 precision instrumentation amplifier. The front-end amplifier rejects the common-mode voltage while amplifying the small sensor signal. Its matched layout and laser trimmed resistors allow it to provide guaranteed specifications for gain error, gain drift, and common-mode rejection. To minimize leakage current, the high-impedance sensor output can be guarded by sampling the input voltage and connecting the buffered voltage to an unmasked trace around the input signal path.

The first-stage gain is typically 10 to 20, but not higher, because the low-level signal must be amplified for postprocessing while the dc offset is kept small to avoid saturating downstream stages.

The input stage is followed by an active band-pass filter that removes the dc component and sets the gain to fully use the dynamic range of the downstream ADC. The sensor excitation frequency ranges between 1⁄25 and 1⁄2 of the power line frequency, setting the band-pass cutoff frequencies. Figure 9 shows the band-pass filter used in the flow meter.

The first stage is an ac-coupled unity-gain high-pass filter with 0.16 Hz cutoff frequency. Its transfer function is

$$H(\omega) = \frac{j\omega R_{91}C}{1 + j\omega R_{91}C} \cdot \left(1 + \frac{R_{97}/R_{98}}{1 + j\omega R_{97}C_{162}}\right) \cdot \frac{j\omega R_{94}C_{152}}{1 + j\omega R_{94}C_{152}} \cdot \frac{-R_{95}/R_{89}}{1 + j\omega R_{95}C_{160}}$$

The following stages combine with the first to form a complete band-pass filter with 0.37-Hz low-frequency cutoff, 37-Hz high-frequency cutoff, 35.5-dB peak at 3.6 Hz, –40 dB/decade roll off, and 49-Hz noise equivalent bandwidth. The amplifier chosen for this stage must not contribute additional system noise.

Using the AD8622 low-power precision op amp, which specifies 0.2 μV_{P-P} 1/f noise and 11 nV/√Hz wideband noise, the noise referred to the filter input is 15 nV rms. When referred to the amplifier input, this noise becomes 1.5 nV rms, which can be ignored compared to the ±1.5 μV_{P-P} noise for 1 m/s flow rate. Adding together the noise sources from the common-mode voltage, front-end amplifier, and band-pass filter, the root-sum-square noise referred to the AD8228 input is 0.09 µV rms, or about 0.6 μV_{P-P}.

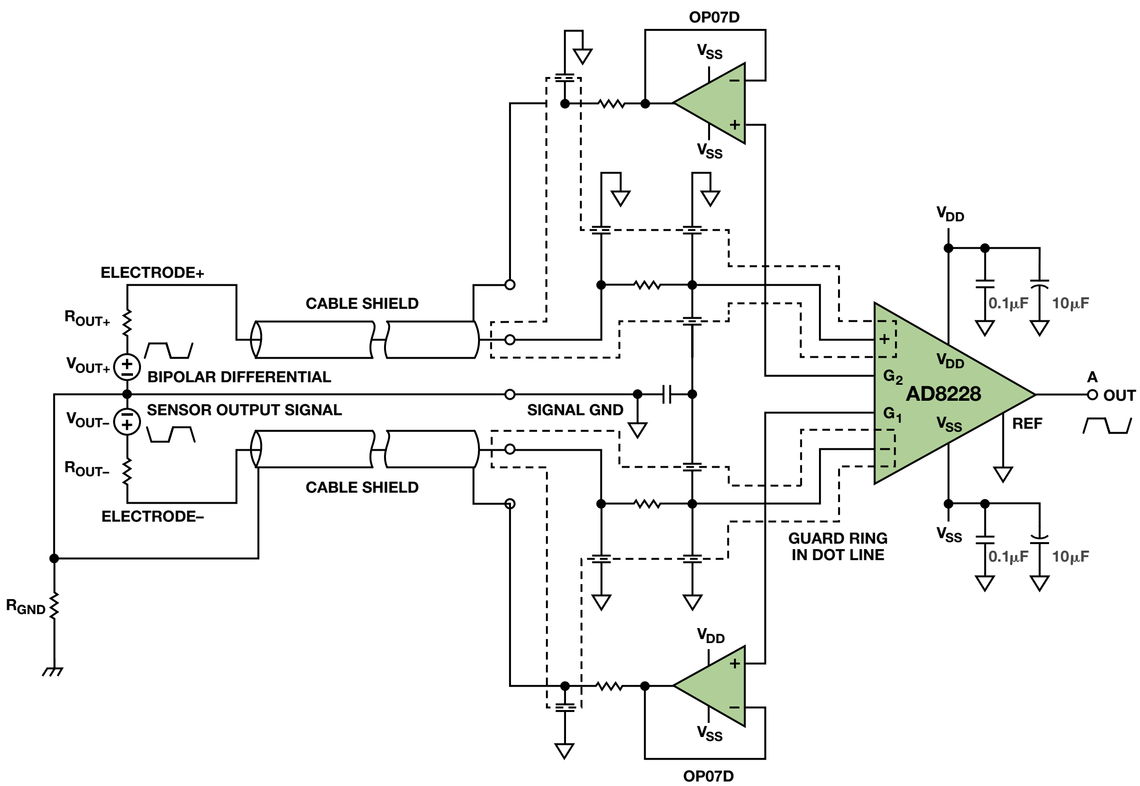

Figure 8. Interface between front-end amplifier and electromagnetic flow sensor.

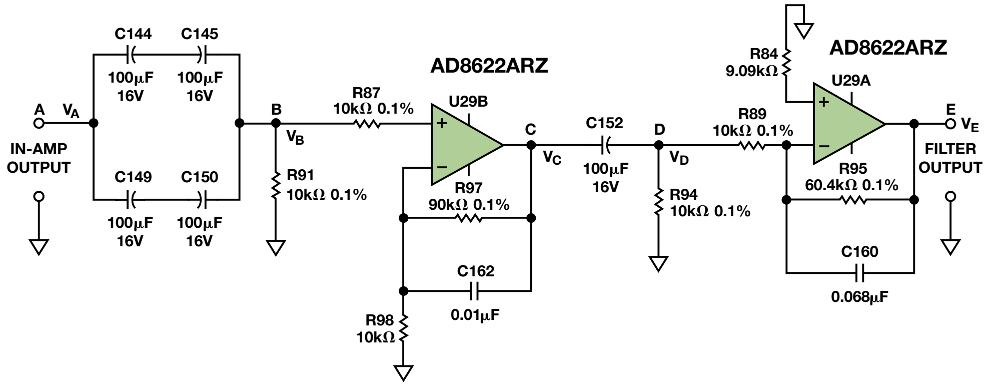

Figure 9. Band-pass filter following the input amplifier.

The filter output contains the flow rate in the amplitude and the flow direction in the phase. The bipolar signal is demodulated with analog switches, hold capacitors, and a difference amplifier, as shown in Figure 10. The analog switches must have low on resistance and medium switching speed. The ADG5412 high-voltage, latch-up proof, quad SPST switches, which feature 9.8 Ω typical R_{ON} and 1.2 Ω R_{ON} flatness, add little gain error or distortion to the signal.

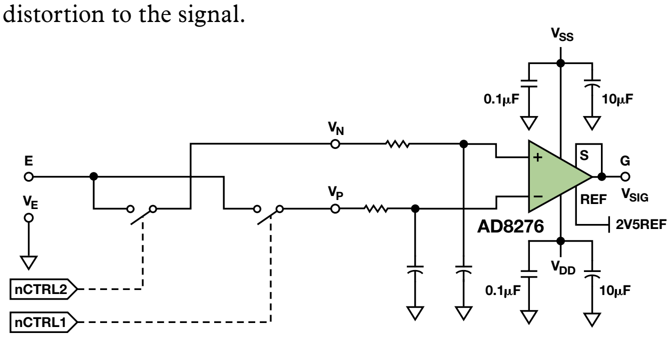

Figure 10. Synchronous demodulation circuit.

The AD8276 low-power, low-cost, unity-gain difference amplifier interfaces to an ADC with a 5-V full scale input range. Thus, its REF pin is tied to a 2.5-V reference that level shifts the bipolar output to a unipolar range. Outputs above 2.5 V represent forward flow, while outputs below 2.5 V represent reverse flow.

Selecting the ADC

When determining system error budgets, the sensor generally dominates, and may account for 80% to 90% of the total error. The international standard for electromagnetic flow meters specifies that measurement repeatability should not exceed ⅓ of the maximum system deviation at 25°C and constant flow rate. With a total error budget of 0.2%, the repeatability should not exceed 0.06%. If the sensor accounts for 90% of this budget, the transmitter electronics must have a maximum error of 60 ppm.

To minimize errors, we can average ADC samples. For example, for every five samples, discard the maximum and minimum, and average the remaining three. The ADC would need to get five samples during each settled interval, which occurs during the final 10% of the excitation period. This requires the ADC sampling rate to be at least 50 times the sensor excitation frequency. To accommodate the fastest excitation of 30 Hz, the minimum sampling rate needs to be 1500 Hz. Faster sampling would allow more data samples to be averaged to suppress noise and achieve better accuracy.

These ADC requirements are ideally suited towards Σ-Δ technology, which delivers excellent noise performance at moderate speeds. The AD7192 ultralow noise Σ-Δ ADC is ideal for electromagnetic flow meters, as it specifies 16.5 bit noise-free resolution at 4800 Hz output data rate. Table 5 shows its effective resolution vs. gain and output data rate.

Figure 11 shows the ADC subcircuit, including the demodulator output and the ADR3425 micropower, high-accuracy 2.5-V reference.

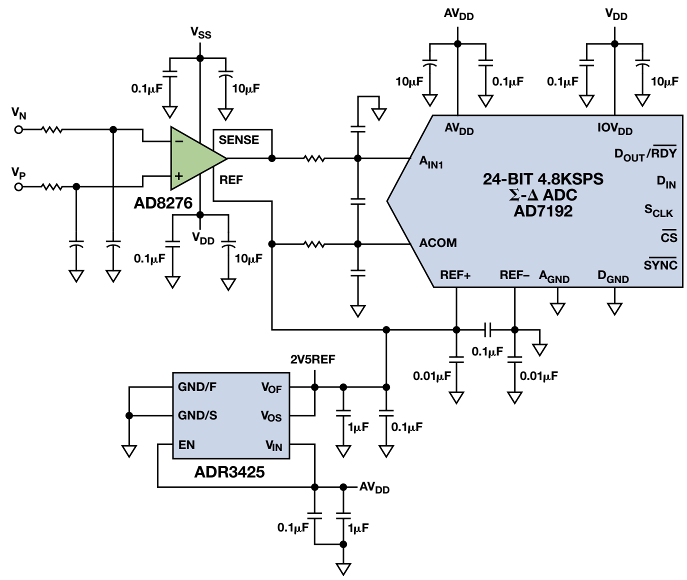

Figure 11. ADC subcircuit.

Some applications, such as beverage filling, need higher frequency sensor excitation. 150 Hz sensor coil excitation allows the filling process to be done in about one second. Noise requirements remain the same, but the ADC must be faster. The AD7176-2 Σ-Δ ADC settles in 20 µs, with 17-bit noise-free resolution at 250 kSPS and 85 dB rejection of 50 Hz and 60 Hz tones.

Table 5. AD7192 Effective Resolution vs. Gain and Output Data Rate

Filter Word (Decimal)	Output Data Rate (Hz)	Settling Time (ms)	Gain of 1[1]	Gain of 8[1]	Gain of 16[1]	Gain of 32[1]	Gain of 64[1]	Gain of 128[1]
1023	4.7	852.5	24 (22)	24 (22)	24 (21.5)	24 (21.5)	23.5 (21)	22.5 (20)
640	7.5	533	24 (22)	24 (21.5)	24 (21.5)	23.5 (21)	23 (20.5)	22.5 (20)
480	10	400	24 (21.5)	23.5 (21)	23.5 (21)	23.5 (21)	23 (20.5)	22 (19.5)
96	50	80	22 (19.5)	22 (19.5)	22 (19.5)	22 (19.5)	21.5 (19)	21 (18.5)
80	60	66.7	22 (19.5)	22 (19.5)	22 (19.5)	21.5 (19)	21.5 (19)	20.5 (18)
40	120	33.3	22 (19.5)	21.5 (19)	21.5 (19)	21.5 (19)	21 (18.5)	20.5 (18)
32	150	26.7	21.5 (19)	21.5 (19)	21.5 (19)	21 (18.5)	21 (18.5)	20 (17.5)
16	300	13.3	21.5 (19)	21.5 (19)	21 (18.5)	21 (18.5)	20.5 (18)	19.5 (17)
5	960	4.17	20.5 (18)	20.5 (18)	20.5 (18)	20 (17.5)	19.5 (17)	19 (16.5)
2	2400	1.67	20 (17.5)	20 (17.5)	19.5 (17)	19.5 (17)	19 (16.5)	18 (15.5)
1	4800	0.83	19 (16.5)	19 (16.5)	19 (16.5)	18.5 (16)	18.5 (16)	17.5 (15)

[1]The output peak-to-peak (p-p) resolution is listed in parenthesis.

Analog Signal Chain Testing

The building blocks described here were used to excite and test an electromagnetic flow sensor in a calibration laboratory. The complete front end, including high CMRR input stage, band-pass filter, and gain stage were also tested in a real flow system. Two test boards achieved ±0.2% accuracy on the 1 m/s to 5 m/s range, with a repeatability of 0.055%. This correlates well with industrial standards. The signal chain for an electromagnetic flow meter is shown in Figure 12.

The sensor excitation and measurement dictates overall system performance, as the millivolt signal developed at the electrodes is ultimately converted into a flow result. The flow rate is communicated to the system controller via several protocols, including RS-485 and a 4-mA to 20-mA current loop. Key advantages of the current loop are that it is not affected by the voltage drop in the wiring, can communicate over long distances, and is less susceptible to noise interference than voltage communications. In factory automation applications, digital bus protocols are more common, offering high-speed communications over shorter distances using a differential voltage mode signal. Figure 13 shows a 4-mA to 20-mA signaling circuit with HART® communications. Figure 14 shows an isolated RS-485 solution.

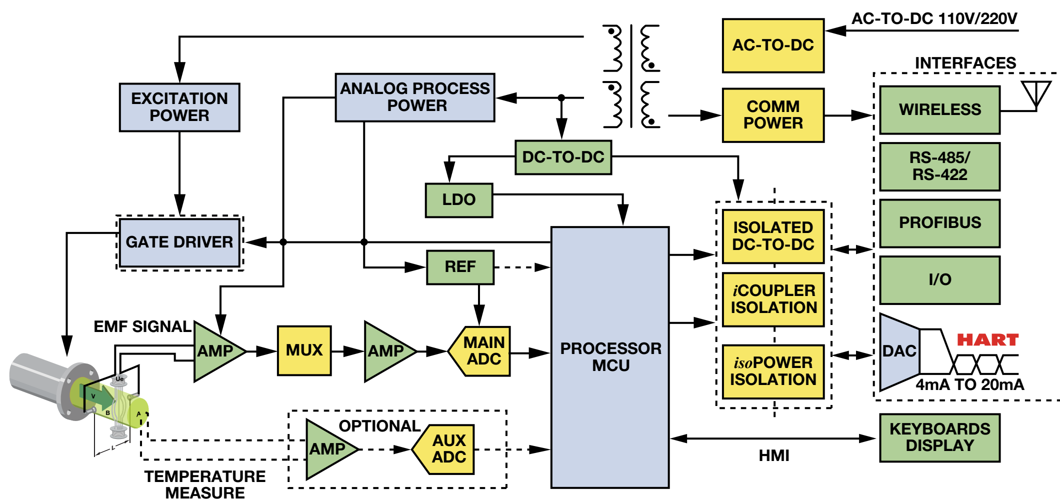

Figure 12. Electromagnetic flow meter.

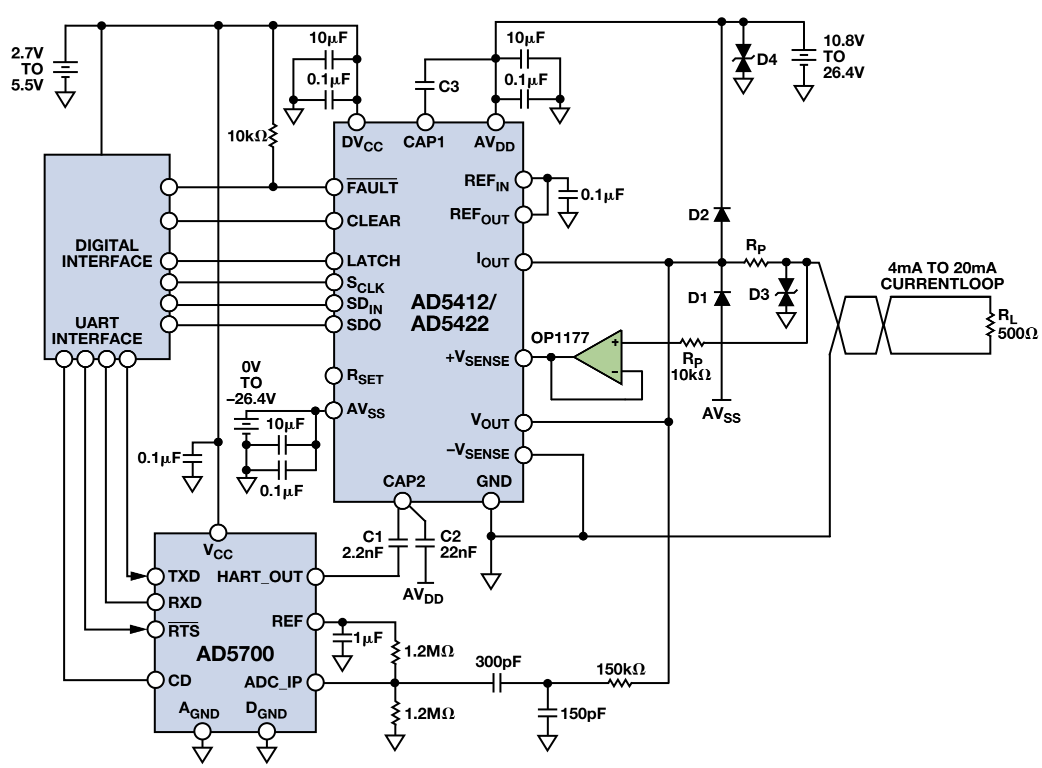

Figure 13. 4-mA to 20-mA current loop with HART.

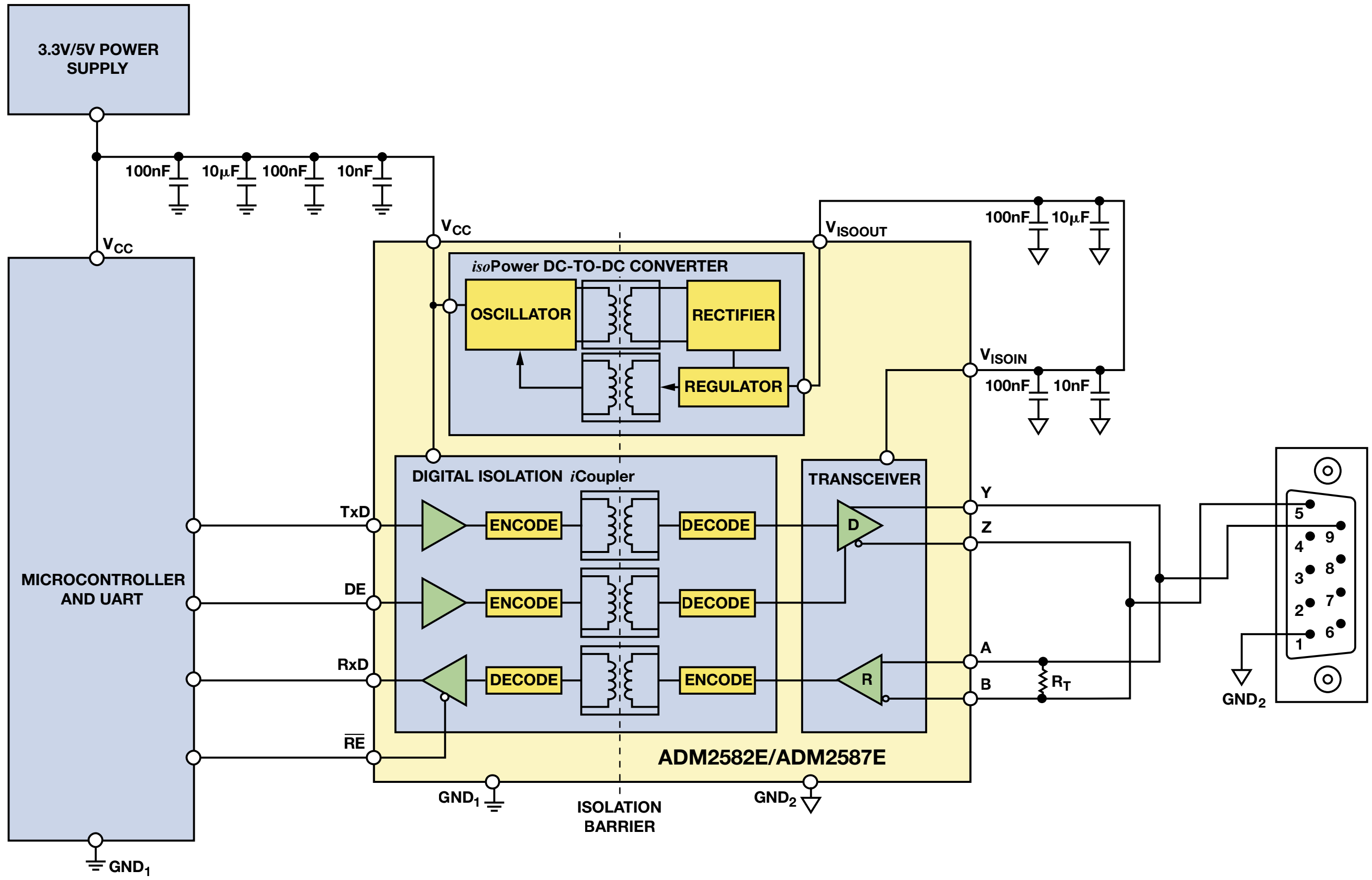

Figure 14. Isolated RS-485 circuit.

To maintain safe voltages at the user interface and to prevent transients from being transmitted from the sources, galvanic isolation is usually required between each communication channel and the system controller. Table 6 shows a list of components that provide the highest levels of integration for these communications standards.

Table 6. Integrated Circuits for Industrial Data Acqusition

Output	Solution	Description	Advantages
4-mA to 20-mA	AD5410/AD5420	Single-Channel, 16-Bit, Current Source DAC	Open/short diagnostics. Over-temperature fault Output slew rate control Software-programmable current/voltage ranges
4-mA to 20-mA	AD5412/AD5422	Single-Channel, 16-Bit, Current Source and Voltage Output DAC, HART Connectivity	Open/short diagnostics. Over-temperature fault Output slew rate control Software-programmable current/voltage ranges
4-mA to 20-mA	AD5750	Industrial Current/Voltage Output Driver with Programmable Ranges	Open/short diagnostics. Over-temperature fault Output slew rate control CRC error checking Negative current ranges
HART	AD5700	Low-Power HART Modem	115 µA maximum supply current in receive mode Integrated band-pass filter Minimal external components
RS-232	ADM3251E	Isolated Single-Channel RS232 Line Driver/Receiver	ESD protection on R_{IN} and T_{OUT} pins ±8 kV: contact discharge ±15 kV: air gap discharge
CAN BUS	ADM3053	2.5 kV rms Signal and Power Isolated CAN Transceiver	Current limiting and thermal shutdown features to protect against output short circuits
RS-485	ADM2582E	2.5 kV Signal and Power Isolated, ±15 kV ESD Protected, Full/Half Duplex RS-485	Open- and short-circuit, fail-safe receiver inputs Thermal shutdown protection

Conclusion

Electromagnetic flow meters are among the most common types of flow technologies used today. They dominate in liquid flow measurement and are particularly popular in Europe due to the focus on waste management systems. The main trends are towards PCB area reduction and higher performance. The system performance is dictated by the analog input block, necessitating a high-impedance, low-noise, high-CMRR input amplifier and a low-noise, high-resolution Σ-Δ ADC. Future trends will dictate the need for even faster ADCs. The AD719x family of ADCs suits current system level requirements, while the AD7176 family is well positioned to meet future requirements. ADI's portfolio of high-efficiency dc-to-dc regulators, integrated communications, high-resolution ADCs, precision amplifiers, and high-accuracy voltage references will allow designers to exceed these requirements in new designs.

Authors

Li Ke [ke.li@analog.com] joined Analog Devices in 2007 as an applications engineer with the Precision Converters product line, located in Shanghai, China. Previously, he spent four years as an R&D engineer with the Chemical Analysis group at Agilent Technologies. Li received a master's degree in biomedical engineering in 2003 and a bachelor's degree in electric engineering in 1999, both from Xi'an Jiaotong University. He has been a professional member of the Chinese Institute of Electronics since 2005.

Colm Slattery [colm.slattery@analog.com] graduated in 1995 from the University of Limerick, Ireland, with a bachelor's degree in electronic engineering. After working in test development engineering at Microsemi, he joined Analog Devices in 1998. He spent three years in an applications role in Shanghai and is currently working as a system applications engineer for the Industrial and Instrumentation segment.